ChemComm

Synthesis and electrochemical properties of Li1.3Nb0.3Cr0.4O2 as a high-capacity cathode material for rechargeable Lithium batteries

Journal:	*ChemComm*
Manuscript ID	CC-COM-09-2018-007660.R1
Article Type:	Communication

Journal Name

COMMUNICATION

Synthesis and electrochemical properties of $Li_{1.3}Nb_{0.3}Cr_{0.4}O_2$ as a high-capacity cathode material for rechargeable Lithium batteries

Received 00th January 20xx,
Accepted 00th January 20xx

DOI: 10.1039/x0xx00000x

www.rsc.org/

Weiwen Wang,[a] Jingke Meng,[b] Xinyang Yue,[b] Qinchao Wang,[b] Xinxin Wang,[b] Yongning Zhou,[b] Zhengwen Fu*[a] and Zulipiya Shadike*[c]

A cation-disordered Li-excess cathode material on a binary system for xLi_3NbO_4-(1-x)$LiCrO_2$ (x = 0.43) have been successfully prepared by mechanical milling, delivers a highly reversible capacity of ~362 mAh g^{-1}, which originates from a highly reversible Cr^{3+}/Cr^{6+} three-electron redox reaction with electrochemically inactive niobium ions.

With increasing demand for high-energy-density Li-ion batteries, great efforts have been made by using diverse high capacity and/or high voltage cathode materials.[1-3] In particular, oxide-based materials have been extensively studied over the past decade, as they tend to deliver the highest energy densities.[4-6] Significant breakthroughs will be most likely to come from deviations from the current exemplification of well-layered oxides with one-electron transition-metal oxidation, such as $LiCoO_2$ and $LiMn_2O_4$, because these materials have been fully explored. Recently, so called Li-rich manganese layered oxides, Li_2MnO_3 and its derivatives have drawn the special attention in the field of high-capacity cathode materials.[7, 8] Historically, Li_2MnO_3 had been originally thought to be electrochemically inactive because oxidation of Mn ions beyond the tetravalent state is difficult. However, the fact is that Li_2MnO_3 is electrochemically active, presumably due to charge compensation by negatively oxide ions, instead of conventional transition metal ions (e.g. Mn^{3+}/Mn^{4+}). Theoretical[9, 10] and experimental[11] studies for the Li-rich system have revealed that oxide ions as anionic species can also participate in the charge compensation process. However, in spite of the impressive success in achieving such high capacity (250 ~ 300 mAh g^{-1}), irreversible structural changes during electrochemical cycles, which are associated with partial oxygen loss on charge, will inevitable plague its use for practical applications.[12] As enormous progress has been made in the oxide space, enlarging the search space of high-energy-density cathode materials to cation-disordered lithium transition metal oxides (Li-TM oxides). Cation-disordered materials, in a very long time, have been disregarded as electrode materials because they generally result in poor electrochemical performance as cation mixing will mostly reduce the Li layer spacing (Li slab distance) and subsequently block Li diffusion channel.[13] But recent breakthroughs with disordered Li-excess electrode materials (x > 0.1 in $Li_{1+x}TM_{1-x}O_2$) and percolation theory have regained extreme attention in this field.[4, 5, 14-16]

Herein, chromium ions (Cr^{3+}) are first substituted for Li^+ and Nb^{5+} ions in Li_3NbO_4 based on a binary system for xLi_3NbO_4-(1-x)$LiCrO_2$. A single phase with nanosized (50 ~ 200 nm) was successfully obtained for x = 0.43, which corresponds to $Li_{1.3}Cr_{0.4}Nb_{0.3}O_2$. Approximately 362 mAh g^{-1} of reversible capacity can be delivered with small charge/discharge polarization, even though the $Li_{1.3}Nb_{0.3}Cr_{0.4}O_2$ sample crystallizes into the cation-disordered rocksalt-type structure. The electrochemical performance of $Li_{1.3}Nb_{0.3}Cr_{0.4}O_2$ was found to be much better than that of $LiCrO_2$ with the layered structure. Chromium ions are oxidized/reduced reversibly based on three electron redox (Cr^{3+}/Cr^{6+}) in $Li_{1.3}Nb_{0.3}Cr_{0.4}O_2$ during the electrochemica process, which is consistent with the observed reversible capacity of $Li_{1.3}Nb_{0.3}Cr_{0.4}O_2$ electrode in Li batteries.

Similar to Li_2MnO_3, the crystal structures of Li_3NbO_4 is also classified as cation-ordered rocksalt superstructures (Fig. 1a).[17] However, Li_3NbO_4 is electrochemically inactive (Fig. S1) because no electron existed in the conduction band ($4d^0$ configuration for Nb^{5+}), even though it crystallizes into the lithium-excess rocksalt structure.[16, 18] As it is known, a crystal structure of $LiCrO_2$ without niobium ions is assigned as the conventional layered structure like highly active $LiCoO_2$, however, it shows almost no signs of reversible lithium intercalation (Fig. S1).[19, 20] The crystal structures of Li_3NbO_4 and $LiCrO_2$ are all classified as rocksalt-type superstructures, indicating that both oxides

[a] Department of Chemistry, Shanghai Key Laboratory of Molecular Catalysis and Innovative Materials, Fudan University, Shanghai 200433, P. R. China.
[b] Department of Materials Science, Fudan University, Shanghai 200433, P. R.China.
[c] Chemistry Division, Brookhaven National Laboratory, Upton, New York, 11973, USA.
E-mail: zwfu@fudan.edu.cn, zshadike@bnl.gov
† Footnotes relating to the title and/or authors should appear here.
Electronic Supplementary Information (ESI) available: [details of any supplementary information available should be included here]. See DOI: 10.1039/x0xx00000x

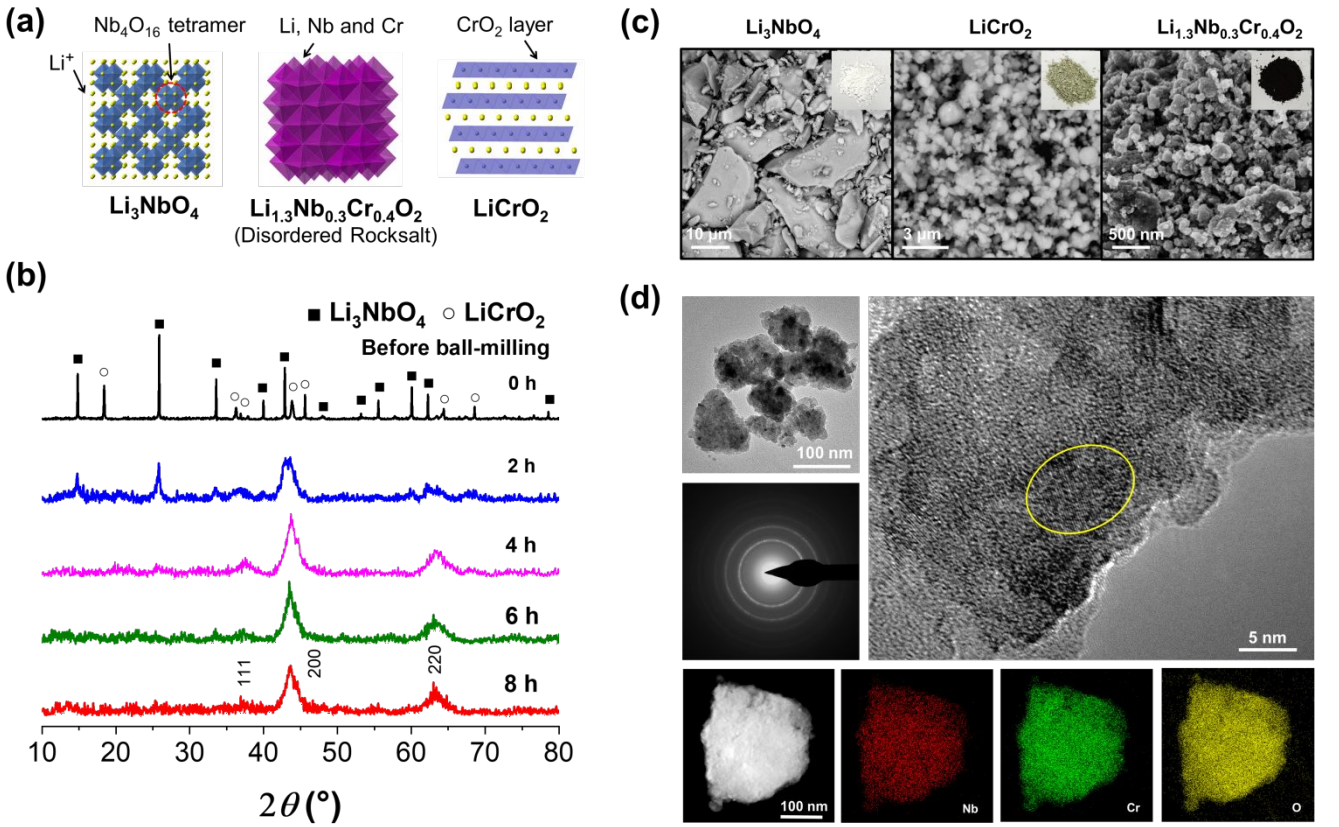

Fig. 1 (a) Schematic of the crystal structures of Li_3NbO_4, $Li_{1.3}Nb_{0.3}Cr_{0.4}O_2$, and $LiCrO_2$. (b) X-ray diffraction patterns of a mixture of Li_3NbO_4 and $LiCrO_2$ before and after the mechanical milling. (c) Particle morphology observed by SEM, Li_3NbO_4, $Li_{1.3}Nb_{0.3}Cr_{0.4}O_2$, and $LiCrO_2$. The insert is the photographs of the sample powders with different colors. (d) TEM images, an electron diffraction pattern and STEM/EDX mapping images of $Li_{1.3}Nb_{0.3}Cr_{0.4}O_2$.

consist of a common cubic close-packed (ccp) oxygen lattice, and the difference is only existed in cation distribution in octahedral sites. Therefore, the formation of solid solution samples is expected in a binary system for $x$$Li_3NbO_4$-(1-$x$)$LiCrO_2$. A single phase has been successfully obtained as $Li_{1.3}Nb_{0.3}Cr_{0.4}O_2$, which corresponds to x = 0.43 in Li_3NbO_4-(1-x)$LiCrO_2$. Clustering of niobium ions is disturbed in this binary system, forming the cation-disordered rocksalt structure.

Nevertheless, our trial to synthesize samples by conventional calcination failed (Fig. S2). Phase segregation into Li_3NbO_4 and $LiCrO_2$ has been evidenced, and a narrow solid solution range is anticipated in this binary system. $Li_{1.3}Nb_{0.3}Cr_{0.4}O_2$ was not identified as a thermodynamically stable phase. Therefore, an alternate route was selected, i.e., synthesis of a metastable phase, and mechanical milling has been chosen in this study. Fig. 1b shows X-ray diffraction patterns of the samples before and after the mechanical milling. The diffraction lines of $LiCrO_2$ and Li_3NbO_4 in a 2θ range of 10-70° gradually disappear under mechanical milling, and new peaks appear at 38, 43.5, and 63°, which are assigned as a cation-disordered rocksalt structure. This fact indicates that a mixture of Li_3NbO_4 and $LiCrO_2$ is gradually changed into the cation-disordered rocksalt structure, in which all ions are located in the same octahedral sites of the ccp lattice. A single-phase sample is obtained after milling for 8 h.

Particle morphology of the samples was observed by scanning electron microscope (SEM) and transmission electron microscope (TEM). From SEM images in Fig. 1c, the primary particle size of the as-prepared $Li_{1.3}Nb_{0.3}Cr_{0.4}O_2$ should be ranged from 50 to 200 nm, which is much smaller than that of $LiCrO_2$ and Li_3NbO_4 (approximately 2 μm and 15 μm, respectively). The electrode performance of Li_3NbO_4-based electrode materials is known to depend on the primary particle size, which originates from the slow kinetics for the oxidation of oxide ion.[18] Besides, substitution of 3*d* transition metal ions for Nb/Li ions can effectively induce conductive electrons, and color of samples is also changed from white for Li_3NbO_4 to black for substituted samples with Cr^{3+} after the mechanical milling. The black color of the electrode materials usually means good conductivity, which is vital to insure excellent electrode performance. With reduced particle size and improved electrical conductivity, the electrochemical performance of $Li_{1.3}Nb_{0.3}Cr_{0.4}O_2$ is worth expecting. TEM shows that the primary particles are polycrystalline and made of crystalline grains about 10 nm in size, as the electron diffraction pattern consists of a series of diffraction rings and clear lattice fringes are noted in Fig. 1d). No amorphous components were detected in TEM, indicating that the electrochemical properties are predominantly determined by the $Li_{1.3}Nb_{0.3}Cr_{0.4}O_2$ phase. Energy-dispersive X-ray elemental mapping (EDX) on a $Li_{1.3}Nb_{0.3}Cr_{0.4}O_2$ particle, conducted by scanning transmission electron microscopy (STEM), reveals a homogeneous distribution of Nb, Cr and O, at least at the level of the resolution of STEM scanning (~0.20 nm). Additionally, chemical

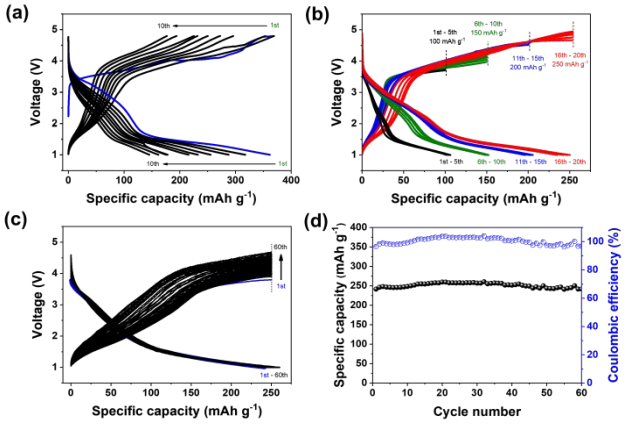

Fig. 2 (a) Galvanostatic charge/discharge profiles of $Li_{1.3}Nb_{0.3}Cr_{0.4}O_2$ at a rate of 10 mA g^{-1} in the voltage range of 1.0-4.8 V. (b) Voltage-capacity profiles of $Li_{1.3}Nb_{0.3}Cr_{0.4}O_2$ with constant charge capacity (100, 150, 200, and 250 mAh g^{-1}) at a rate of 10 mA·g^{-1}. (c) Voltage-capacity profiles and (d) cycling performance of $Li_{1.3}Nb_{0.3}Cr_{0.4}O_2$ with constant charge capacity of 250 mAh g^{-1} at a rate of 10 mA·g^{-1}.

compositions of the as-prepared $Li_{1.3}Nb_{0.3}Cr_{0.4}O_2$ obtained from EDX spectra are consistent with the nominal composition , as demonstrated in Fig. S3 and Table S1.

The electrode performance of $Li_{1.3}Nb_{0.3}Cr_{0.4}O_2$ is shown in Fig. 2a in the voltage range of 1.0-4.8 V at ambient temperature. The $Li_{1.3}Nb_{0.3}Cr_{0.4}O_2$ sample exhibits high initial charge/discharge capacity of ~368/362 mAh g^{-1}, which are close to the theoretical capacity (388 mAh g^{-1}) of $Li_{1.3}Nb_{0.3}Cr_{0.4}O_2$ if all lithium ions are extracted/inserted reversibly from/into the crystal lattice (Fig. S1). Such high reversible capacity of the electrode materials is the highest among the reported binary systems between Li_3NbO_4 and $LiMeO_2$ (MeO).[16, 21] However, the cyclability as electrode materials with galvanostatic charge/discharge is not ideal with capacity fade rapidly, need further improvement. The improved cyclability was realized by charge with a constant capacity mode. Charge capacities were stepwisely increased from 100 to 250 mAh g^{-1} by 50 mAh g^{-1} after each five cycles. Typical discharge profiles at 10 mA g^{-1} with different charge capacities are shown in Fig. 2b. Excellent capacity retention is observed even at a charge capacity of 250 mAh g^{-1}. And the reversible limit of $Li_{1.3}Nb_{0.3}Cr_{0.4}O_2$ as electrode materials is estimated to be ~250 mAh g^{-1} in this experimental condition, mainly restricted by the decomposition of the electrolyte at high voltage.[22] Therefore, a continuous cycle test was performed by charge with constant capacity of 250 mAh g^{-1}. As shown in Fig. 2c, cycling performance of $Li_{1.3}Nb_{0.3}Cr_{0.4}O_2$ was obviously improved by constant capacity charge. The sample demonstrates a stable discharge profiles with ~250 mAh g^{-1} of reversible capacity (~99% of coulombic efficiency) for more than 60 cycles (Fig. 2d), even though initial discharge capacity was slightly low (241 mAh g^{-1}) and a gradual increase in charge polarization was observed.

The XAS spectra of Cr and Nb at K-edge were collected for $Li_{1.3}Nb_{0.3}Cr_{0.4}O_2$ with different oxidation/reduction conditions to clarify the redox species on the oxidation/reduction processes (Fig. 3a). From Cr K-edge (mainly dipole transition from 1s core-level to empty 4p level) spectra, as shown in Fig. 3b and S4, energy position of spectra for the as-prepared sample is similar to that of Cr_2O_3 and $LiCrO_2$ containing trivalent chromium ions.[15] The spectra clearly shift to a higher-energy region on charge as increase in charge capacities. Additionally, the increase in area for a pre-edge peak at ~5994 eV was found in the XAS spectra. The prominent pre-edge peak formed appered during the charging process is a strong evidence of Cr^{6+} formation and migration of Cr^{6+} ions to tetrahedral sites. In the case of tetrahedral symmetry, the strong pre-edge peak mainly originates from an electric dipole transition from the 1s to p components, which are hybridized with 3d-orbitals for chromium ions.[23] Besides, the pre-edge peaks by the electric dipole transition are often intensified by a decrease in the number of d-orbital electrons.[24] The spectrum of the fully charged sample (386 mAh g^{-1}) resembles that of the CrO_3 (Cr^{6+}) reference material. (Fig. S4). So, by considering the large reversible capacity and change in the profile of Cr K-edge spectra, trivalent chromium ions (Cr^{3+}) in $Li_{1.3}Nb_{0.3}Cr_{0.4}O_2$ are oxidized to a higher oxidation state, ~Cr^{6+}, after fully charged. This is consistent with the previous reports about the Cr^{3+}/Cr^{6+} redox process.[15, 25, 26] Chromium often occurs as Cr^{3+} or Cr^{6+} ions in its oxygen-based compounds. The larger Cr^{3+} ion (2.01 Å) tends to prefer octahedral coordination, while the smaller Cr^{6+} ion (1.64 Å) prefers tetrahedral coordination with oxygen.[27] Similar to a solid solution of Li_2MnO_3-$LiCrO_2$ ($Li_{1.2}Cr_{0.4}Mn_{0.4}O_2$), when it was electrochemically oxidized, Cr^{3+} was oxidized into Cr^{6+}, simultaneously, chromium is migrated from the original octahedral site to the interstitial tetrahedral site in the interslab

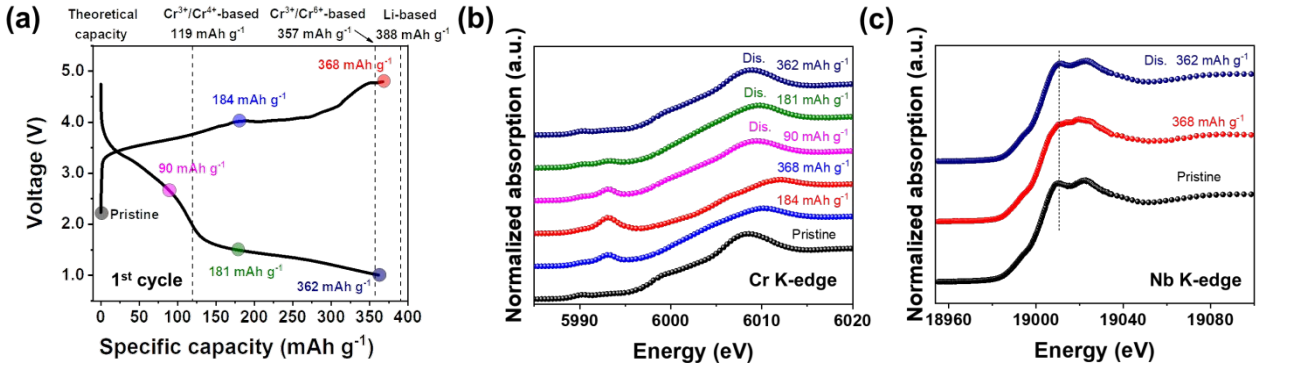

Fig. 3 (a) Galvanostatic charge/discharge profiles of $Li_{1.3}Nb_{0.3}Cr_{0.4}O_2$ at a rate of 10 mA g^{-1} in the range of 1.0-4.8 V during the first cycle, the points on the profiles stand for the states where X-ray absorption spectra (XAS) data were collected. XAS spectra at the (b) Cr and (c) Nb K-edges of the $Li_{1.3}Nb_{0.3}Cr_{0.4}O_2$ samples at different charge/discharge states.

space. Indeed, reversible Cr^{6+} migration has been observed in $Li_{1.2}Cr_{0.4}Mn_{0.4}O_2$ during electrochemical cycling using *in situ* X-ray absorption spectroscopy.[25] It is also worthy to note that chromium ions are reduced reversibly to a trivalent state after discharge to 1.0 V, as the oxidation state of Cr for the fully discharged state is found to be almost the same as that of the as-prepared sample. No change in the absorption edge and peak position of niobium ion is observed even at the full discharged state, as shown in Fig. 3c, indicating that Nb oxidation state is found to be not affected by charge/discharge process even though peak profile is slightly changed by charge process. This fact shows that niobium ions are stabilized at pentavalent state and are not reduced by discharge process, indicating that niobium ions are not responsible for the large discharge capacity of $Li_{1.3}Nb_{0.3}Cr_{0.4}O_2$ as the redox center. Additionally, based on the observed reversible capacity, the contribution of oxide ions is not evidenced in the chromium system. Moreover, it needs to be pointed out that the mechanical milling process will result in the formation of nanosized particles, highly increased specific surface area and the samples contain many grain boundaries. Thus, contributions of surface conversion[28] and interfacial charge storage[29] to reversible capacities cannot be ignored. Further studies of the reaction mechanisms are currently in progress in our group.

In summary, a cation-disordered rocksalt Li-excess cathode material on a binary system for xLi_3NbO_4-(1-x)$LiCrO_2$ have been successfully prepared by mechanical milling. A single phase, obtained for x = 0.43 ($Li_{1.3}Cr_{0.4}Nb_{0.3}O_2$), shows large reversible capacities of ~362 mAh g^{-1}, which originates from a highly reversible Cr^{3+}/Cr^{6+} three-electron redox reaction with electrochemically inactive niobium ions (Nb^{5+}). Moreover, excellent capacity retention as electrode material was confirmed by charge with constant capacity of 250 mAh g^{-1}. A relatively stable coulombic efficiency of ~99% and negligible capacity loss waswere demonstrated for over 60 cycles. These findings will contribute to the development of high-energy-density cation-disordered Li-excess cathode materials for rechargeable Li batteries in the future.

This work was financially supported by the National Natural Science Foundation of China (Grant No. 21773037), National Key Scientific Research Project (Grant No. 2016YFB0901504). In addition, the work at Brookhaven National Laboratory was supported by the Assistant Secretary for Energy Efficiency and Renewable Energy, Vehicle Technology Office of the U.S. Department of Energy through the Advanced Battery Materials Research (BMR) Program, including Battery500 Consortium under contract DE-SC0012704.

Conflicts of interest

There are no conflicts to declare.

Notes and references

1 J. W. Choi and D. Aurbach, *Nature Reviews Materials*, 2016, **1**, 16013.
2 S. Hy, H. Liu, M. Zhang, D. Qian, B. Hwang and Y. S. Meng, *Energy Environ. Sci*, 2016, **9**, 1931-1954.
3 J. Shi, D. Xiao, M. Ge, X. Yu, Y. Chu, X. Huang, X. Zhang, Y. Yin, X. Yang, Y. Guo, L. Gu and L. Wan, *Adv. Mater.*, 2018, 1705575.
4 A. J. Perez, Q. Jacquet, D. Batuk, A. Iadecola, M. Saubanère, G. Rousse, D. Larcher, H. Vezin, M. Doublet and J. Tarascon, *Nature Energy*, 2017, **2**, 954-962.
5 J. Lee, A. Urban, X. Li, D. Su, G. Hautier and G. Ceder, *Science*, 2014, **343**, 519-522.
6 K. Kang, Y. S. Meng, J. Breger, C. P. Grey and G. Ceder, *Science*, 2006, **311**, 977-980.
7 C. Zhao, Q. Wang, Y. Lu, Y. Hu, B. Li and L. Chen, *J. Phys. D Appl. Phys.*, 2017, **50**, 83001.
8 A. D. Robertson and P. G. Bruce, *Chem. Commun.*, 2002, 2790-2791.
9 M. Sathiya, G. Rousse, K. Ramesha, C. P. Laisa, H. Vezin, M. T. Sougrati, M. Doublet, D. Foix, D. Gonbeau, W. Walker, A. S. Prakash, M. Ben Hassine, L. Dupont and J. Tarascon, *Nat. Mater.*, 2013, **12**, 827-835.
10 A. Abdellahi, A. Urban, S. Dacek and G. Ceder, *Chem. Mater.*, 2016, **28**, 3659-3665.
11 R. Wang, X. He, L. He, F. Wang, R. Xiao, L. Gu, H. Li and L. Chen, *Adv. Energy Mater.*, 2013, **3**, 1358-1367.
12 J. Rana, M. Stan, R. Kloepsch, J. Li, G. Schumacher, E. Welter, I. Zizak, J. Banhart and M. Winter, *Adv. Energy Mater.*, 2014, **4**, 1300998.
13 M. Obrovac, *Solid State Ionics*, 1998, **112**, 9-19.
14 G. Wei, X. Lu, F. Ke, L. Huang, J. Li, Z. Wang, Z. Zhou and S. Sun, *Adv. Mater.*, 2010, **22**, 4364-4367.
15 Y. Lyu, N. Zhao, E. Hu, R. Xiao, X. Yu, L. Gu, X. Yang and H. Li, *Chem. Mater.*, 2015, **27**, 5238-5252.
16 N. Yabuuchi, M. Nakayama, M. Takeuchi, S. Komaba, Y. Hashimoto, T. Mukai, H. Shiiba, K. Sato, Y. Kobayashi, A. Nakao, M. Yonemura, K. Yamanaka, K. Mitsuhara and T. Ohta, *Nat. Commun.*, 2016, **7**, 13814.
17 K. Ukei, H. Suzuki, T. Shishido and T. Fukuda, *Acta Crystallographica*, 1994, **50**, 655-656.
18 N. Yabuuchi, M. Takeuchi, M. Nakayama, H. Shiiba, M. Ogawa, K. Nakayama, T. Ohta, D. Endo, T. Ozaki, T. Inamasu, K. Sato and S. Komaba, *Proceedings of the National Academy of Sciences*, 2015, **112**, 7650-7655.
19 S. Komaba, C. Takei, T. Nakayama, A. Ogata and N. Yabuuchi, *Electrochem. Commun.*, 2010, **12**, 355-358.
20 S. Miyazaki, S. Kikkawa and M. Koizumi, *Synthetic Met.*, 1983, **6**, 211-217.
21 S. Hoshino, A. M. Glushenkov, S. Ichikawa, T. Ozaki, T. Inamasu and N. Yabuuchi, *ACS Energy Letters*, 2017, **2**, 733-738.
22 N. Choi, J. Han, S. Ha, I. Park and C. Back, *RSC Adv.*, 2015, **5**, 2732-2748.
23 F. de Groot, G. Vanko and P. Glatzel, *J Phys Condens Matter*, 2009, **21**, 104207.
24 T. Yamamoto, *X-Ray Spectrom.*, 2008, **37**, 572-584.
25 M. Balasubramanian, J. McBreen, I. J. Davidson, P. S. Whitfield and I. Kargina, *J. Electrochem. Soc.*, 2002, **149**, A176.
26 Z. Lu and J. R. Dahn, *J. Electrochem. Soc.*, 2003, **150**, A1044.
27 R. D. Shannon, *Acta Crystallographica Section A*, 1976, **32**, 751-767.
28 S. Jung, H. Kim, M. G. Cho, S. Cho, B. Lee, H. Kim, Y. Park, J. Hong, K. Park, G. Yoon, W. M. Seong, Y. Cho, M. H. Oh, H. Kim, H. Gwon, I. Hwang, T. Hyeon, W. Yoon and K. Kang, *Nature Energy*, 2017, **2**.
29 J. Maier, *Nat. Mater.*, 2005, **4**, 805-815.

A table of contents entry

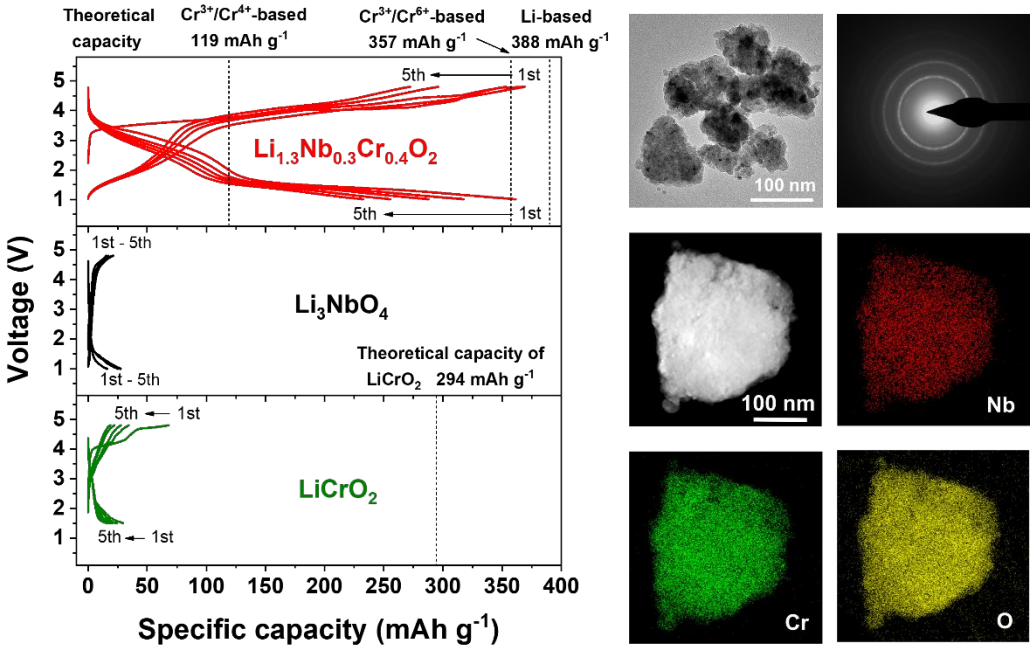

A cation-disordered Li-excess material $Li_{1.3}Cr_{0.4}Nb_{0.3}O_2$ delivers a highly reversible capacity, originating from a Cr^{3+}/Cr^{6+} three-electron redox reaction.